THE JOURNAL OF BIOLOGICAL CHEMISTRY VOL. 280, NO. 39, pp. 33525–33535, September 30, 2005

The Hepatitis B Virus X Protein Sensitizes HepG2 Cells to UV Light-induced DNA Damage*

Received for publication, June 17, 2005, and in revised form, July 29, 2005 Published, JBC Papers in Press, July 30, 2005, DOI 10.1074/jbc.M506628200

Alvin T. C. Lee[‡], Jianwei Ren[‡], Ee-Tsin Wong[§], Kenneth H. K. Ban[§], Linda A. Lee[¶], and Caroline G. L. Lee[‡§1]

From the [‡]Division of Medical Sciences, National Cancer Centre, Singapore 169610, Singapore, the [§]Department of Biochemistry, National University of Singapore, Singapore 119077, Singapore, and the [¶]Department of Medicine, The Johns Hopkins University School of Medicine, Baltimore, Maryland 21287

Various reports have implicated the virally encoded HBx protein as a cofactor in hepatocarcinogenesis. However, direct evidence of the role of HBx as a promoter of oncogenesis in response to an initiating factor such as DNA damage remains inadequate. Here, we report the effects of HBx in HepG2 cells exposed to UV light-induced DNA damage. HBx expression was found not to affect the morphology, viability, and cell cycle/apoptotic profiles or DNA repair machinery of untreated cells. Nonetheless, upon UV treatment, HBx protein levels increased concomitantly with p53 levels. Both HBx and p53 proteins were found to interact and colocalize primarily in the nucleus. The binding of HBx to p53 modulated (but did not inhibit) the transcriptional activation function of p53. Notably, HBx-expressing cells exhibited increased sensitivity to UV damage, resulting in greater G_2/M arrest and apoptosis of these cells. Additionally, these cells displayed a reduced DNA repair capacity in response to UV damage. In conclusion, this work suggests that DNA damage may be an initiating factor in hepatocarcinogenesis and that HBx may act as the promoting factor by inhibiting DNA repair. In hepatitis B virus-infected hepatocytes, a chronic infection may present the opportunity for such a DNA-damaging event to occur, and accumulated errors caused by the inhibition of DNA repair by HBx may result in oncogenesis.

There is compelling evidence showing that the hepatitis B virus (HBV)[2] is a major etiologic factor in hepatocellular carcinoma (HCC) (1). However, the association of chronic HBV infection with HCC is poorly understood. Among the four proteins translated from the HBV genome, the X gene product termed HBx has been implicated in the process of hepatocarcinogenesis.

Mice carrying HBx as a transgene show a direct correlation between the level of HBx expression and the likelihood to develop HCC (2, 3). However, certain lineages of HBx transgenic mice do not exhibit tumor development unless coupled with other factors such as exposure to the hepatocarcinogen diethylnitrosamine (4) or when combined with c-*myc* induction (5). Furthermore, the development of hepatic neoplasia requires the expression of HBx to be above a certain threshold level (3). In addition to the long latent periods usually observed between the time of initial HBV infection and tumor appearance, these observations collectively suggest that HBx does not directly cause cancer but plays a role in liver oncogenesis as a cofactor or tumor promoter. Chronic HBV infection may present a long-term opportunity for an initiating event to occur, and HBx may act by modifying cellular regulatory/control mechanisms facilitating the culmination of the transformation process in the cell.

In this regard, a highly probable tumor-initiating event is DNA damage. Indeed, the effects of HBx on DNA damage repair mechanisms have been proposed as major oncogenic factors. By host cell reactivation assays and unscheduled DNA synthesis studies, HBx has been reported to compromise host cell DNA repair (6–8). The effect of HBx on host cell DNA repair is likely to be due to the interaction between HBx and proteins of the DNA repair complex or p53 (9–11). Normal cells respond to cellular stress events such as DNA damage by increasing intracellular p53 concentrations to induce cell cycle arrest for the repair of damaged DNA. Cells with irreparable damage are usually eliminated by p53-dependent apoptosis (12). However, the role of HBx in regulating apoptosis or its mechanism of regulation remains unclear. HBx has been reported to inhibit (13–15) as well as induce (16–18) apoptosis. The mechanism of regulation of apoptosis by HBx was reported to be via both p53-dependent (19, 20) and p53-independent (21) pathways. p53 was reported to bind to HBx (22) and to localize primarily in the cytoplasm (22–24) in HBx-expressing cells to modulate apoptosis (23). However, it has also been reported that HBx does not colocalize or co-immunoprecipitate with p53 in HBV-infected human liver cells (25).

In cancers (such as HCC) that have a viral etiology, the viruses rarely act as complete oncogenic agents but instead contribute to the development of a transformed cell either as an initiator or a promoter (26). In this study, we directly demonstrate the effect of HBx as an oncogenic promoter in response to UV light-induced DNA damage. Upon UV irradiation, cells expressing HBx had decreased DNA repair capability and nuclear accumulation of functional p53. Cells expressing HBx also showed increased sensitivity to UV damage, exhibiting elevated levels of G_2/M arrest and apoptosis. The ability of HBx to alter the capability of the cell to repair damaged DNA may predispose an individual with chronic HBV infection to cancer, and the long delay in onset of HCC in HBV-infected individuals may be the result of accumulated genetic lesions caused by the inhibition of DNA repair by HBx. Subsequently, a pro-apoptotic effect may exert selective pressure for apoptosis-resistant preneoplastic cells. These observations purport the view that supplementary changes (such as DNA damage) must occur to complement the pleiotropic functions of HBx to disrupt the multiple checkpoints and regulatory mechanisms of a normal cell, thus culminating in malignancy.

* This work was supported by block grants from the National Medical Research Council of Singapore through the National Cancer Centre (to C. G. L. Lee) and from the National Science and Technology Board of Singapore through John Hopkins Singapore (to C. G. L. Lee and L. A. Lee). The costs of publication of this article were defrayed in part by the payment of page charges. This article must therefore be hereby marked "*advertisement*" in accordance with 18 U.S.C. Section 1734 solely to indicate this fact.

[1] To whom correspondence should be addressed: Div. of Medical Sciences, National Cancer Centre, Level 6, Lab 5, 11 Hospital Dr., Singapore 169610, Singapore. Tel.: 65-6436-8353; Fax: 65-6372-0161; E-mail: bchleec@nus.edu.sg.

[2] The abbreviations used are: HBV, hepatitis B virus; HCC, hepatocellular carcinoma; EGFP, enhanced green fluorescence protein; CAT, chloramphenicol acetyltransferase; CMV, cytomegalovirus; NER, nucleotide excision repair; DDB, damaged DNA-binding protein; UV-DDB, UV-damaged DNA-binding protein.

MATERIALS AND METHODS

Recombinant HBx-expressing Adenovirus Preparation—The HBx gene was amplified from pEco63. HBx-expressing (AdHBx) and control (AdControl) recombinant adenoviruses were generated as described previously (27). Briefly, the HBx gene was initially subcloned into the shuttle vector pAdTrack-CMV, and the integrity of the HBx gene in this vector was sequence-verified. Another plasmid containing the adenoviral arms (pAdEasy-1) was cotransformed with either the PmeI-linearized shuttle vector (pAdTract-CMV) or the HBx-containing shuttle vector (pAdTract-CMV-HBx) into *Escherichia coli* BJ5183 cells. Control (pAdControl) and HBx-expressing (pAdHBx) recombinant adenoviral vectors were then generated by homologous recombination of pAdEasy-1 and pAdTract-CMV or pAdTract-CMV-HBx in *E. coli* BJ5183 cells. The colonies obtained were screened for appropriate recombination events by EcoRV and PmeI restriction endonuclease analyses. The pAdControl and pAdHBx vectors (see Fig. 1*A*) were then digested with PacI and transfected into the 293 packaging cell line (which constitutively expresses the E1 gene product) to produce control (AdControl) and HBx-expressing (AdHBx) recombinant adenoviruses. The titer of the virus (expression-forming units/ml) was evaluated by counting the number of fluorescent cells after infection with serially diluted viruses.

Recombinant HBx-expressing Adenovirus Infection and UV Treatment—HepG2 cells were obtained from American Type Culture Collection and maintained at 37 °C in a humidified atmosphere of 5% CO_2 in Dulbecco's modified Eagle's medium supplemented with 10% fetal calf serum. These cells were seeded onto 6-well plates and grown to 40–50% confluency. Recombinant HBx-expressing or vector control adenoviruses were then added at a multiplicity of infection of 5. Twenty-four hours after adenovirus infection, the medium was replaced with fresh Dulbecco's modified Eagle's medium without virus. Cells were observed under a fluorescence microscope to detect enhanced green fluorescence protein (EGFP) fluorescence to assess infection efficiency. Efficiency was noted to be >90% and did not deviate by >5% between experiments. UVC (254 nm) irradiation of infected cells was then performed with a germicidal lamp calibrated to deliver 8 or 16 J/m^2.

Cell Viability—The number of viable uninfected and AdControl- and AdHBx-infected cells was determined by the Cell Titer 96 Aqueous One cell proliferation assay (Promega Corp.) according to the manufacturer's instructions. Cell growth and viability were also monitored at various time points with an Olympus Research inverted microscope (IX51), and images were captured with a QImaging Retiga 1300R digital imager.

Cell Cycle and Apoptosis—Cells were harvested at various time points, washed with phosphate-buffered saline, and fixed in 1% paraformaldehyde or 70% ethanol. These fixed cells were then stained with propidium iodide (Sigma) and analyzed with a FACSCalibur flow cytometer (BD Biosciences) to determine cell cycle profiles. Apoptotic cell death was also assessed by flow cytometry after staining the cells with phycoerythrin-conjugated annexin V and 7-aminoactinomycin D using the Annexin V:PE Apoptosis Detection Kit I (BD Biosciences) or propidium iodide when the DNA content and cell granularity were assessed.

Generation of Anti-HBx Antibody—The HBx open reading frame was cloned into pET16b (Invitrogen). The HBx protein was then overexpressed in bacteria and purified using nickel-nitrilotriacetic acid beads (Qiagen Inc., Hilden, Germany) according to the manufacturer's instructions. Polyclonal antibody against the recombinant HBx protein was then generated in rabbits (Zymed Laboratories Inc.) and purified using an HBx protein column (BioGenes GmbH, Berlin, Germany).

Immunofluorescence Staining—Localization of p53 and HBx proteins was determined by immunofluorescence staining as described previously (28). Briefly, cells grown on glass coverslips were fixed in 2% paraformaldehyde solution and then permeabilized with 0.2% Triton X-100. The cells were co-stained using 1 μg/μl anti-HBx antibody and 1 μg/μl anti-p53 antibody (Santa Cruz Biotechnology, Inc., Santa Cruz, CA) for 1 h at 37 °C. After three washes with phosphate-buffered saline, the coverslips were incubated with Alexa Fluor 647-labeled chicken anti-mouse and Alexa Fluor 488-labeled anti-rabbit IgG secondary antibodies (1:300 dilution; Molecular Probes, Inc., Eugene, OR) for 1 h at room temperature. Cells were also incubated with 4′,6-diamidino-2-phenylindole to distinguish the nucleus. The coverslips were then washed three times with phosphate-buffered saline and mounted on glass slides. The mounted slides were observed with a Zeiss LSM 510 laser scanning confocal microscope.

Immunoprecipitation—Immunoprecipitation was performed using a protein G immunoprecipitation kit (Roche Applied Science) according to the manufacturer's instructions. Briefly, 400 μg (200 μl) of protein from cell lysates was incubated with 2 μg of anti-HBx or anti-p53 antibody at 4 °C for 6 h. A 10-μl bed volume of protein G (provided with the kit) was used per sample. Western blot analysis was performed as described below.

Western Blot Analysis—Equal protein concentrations were electrophoresed on a 12% SDS-polyacrylamide gel and transferred to a polyvinylidene difluoride membrane (Bio-Rad). The blots were then probed with horseradish peroxidase-conjugated anti-p53 antibody (1:10,000 dilution; Santa Cruz Biotechnology, Inc.), goat anti-actin polyclonal antibody (1:30,000 dilution; Santa Cruz Biotechnology, Inc.), or goat anti-HBx polyclonal antibody (1:5000 dilution; generated in this laboratory) for 1 h at room temperature. Horseradish peroxidase-conjugated goat anti-rabbit secondary antibody (1:10,000 dilution; Pierce) was then added to the blots probed with anti-actin or anti-HBx antibody for an additional 1 h at room temperature. Signals on the immunoblots were detected using an enhanced chemiluminescence reagent kit (ECL, Amersham Biosciences).

Real-time Reverse Transcription-PCR—RNA was isolated as described previously (28). cDNA was synthesized from total RNA using SuperScript II reverse transcriptase (Invitrogen) according to the manufacturer's instructions. Real-time PCR was performed with a Rotor-Gene 2000 real-time thermal cycler (Corbett Research, Sydney, Australia) using the QuantiTect™ SYBR Green PCR kit (Qiagen Inc.). Amplification reactions included cDNA template (25 ng), each of the forward and reverse primers for the various genes (0.25 pmol/μl), and 2× PCR Master Mix (5 μl; Qiagen Inc.) in a total volume of 10 μl. The primers for the various genes are as follows: *MDM2*, 5′-TGTAAGTGAACATTCAGGTG-3′ (forward) and 5′-TTCCAATAGTCAGCTAAGGA-3′ (reverse); p21, 5′-CCTCAAATCGTCCAGCGACCTT-3′ (forward) and 5′-CATTGTGGGAGGAGCTGTGAAA-3′ (reverse); *bcl-2*, 5′-TTGGCCCCCGTTGCTT-3′ (forward) and 5′-CGGTTATCGTACCCCGTTCTC-3′ (reverse); *bax*, 5′-TCCCCCCGAGAGGTCTTTT-3′ (forward) and 5′-CGGCCCCAGTTGAAGTTG-3′ (reverse); and β-actin, 5′-ATGTTTGAGACCTTCACACC-3′ (forward) and 5′-AGGTAGTCAGTCAGGTCCCGGCC-3′ (reverse).

Amplification of the transcripts involved an initial denaturation at 95 °C for 15 min, followed by 40 cycles at 95 °C for 30 s, 55 °C for 30 s, and 72 °C for 30 s. SYBR Green fluorescence was measured after each extension step. Standard curves were generated using serially diluted plasmids in which the respective cDNAs were cloned. The linear ranges for the expression of all respective genes were determined to be between 10^3 and 10^8 copies (r^2 = 0.9997 for p21, 0.9994 for *MDM2*, 0.9958 for *bcl-2*, 0.9986 for *bax*, and 0.992 for β-actin). The expression levels of these various genes were then normalized against the expression levels

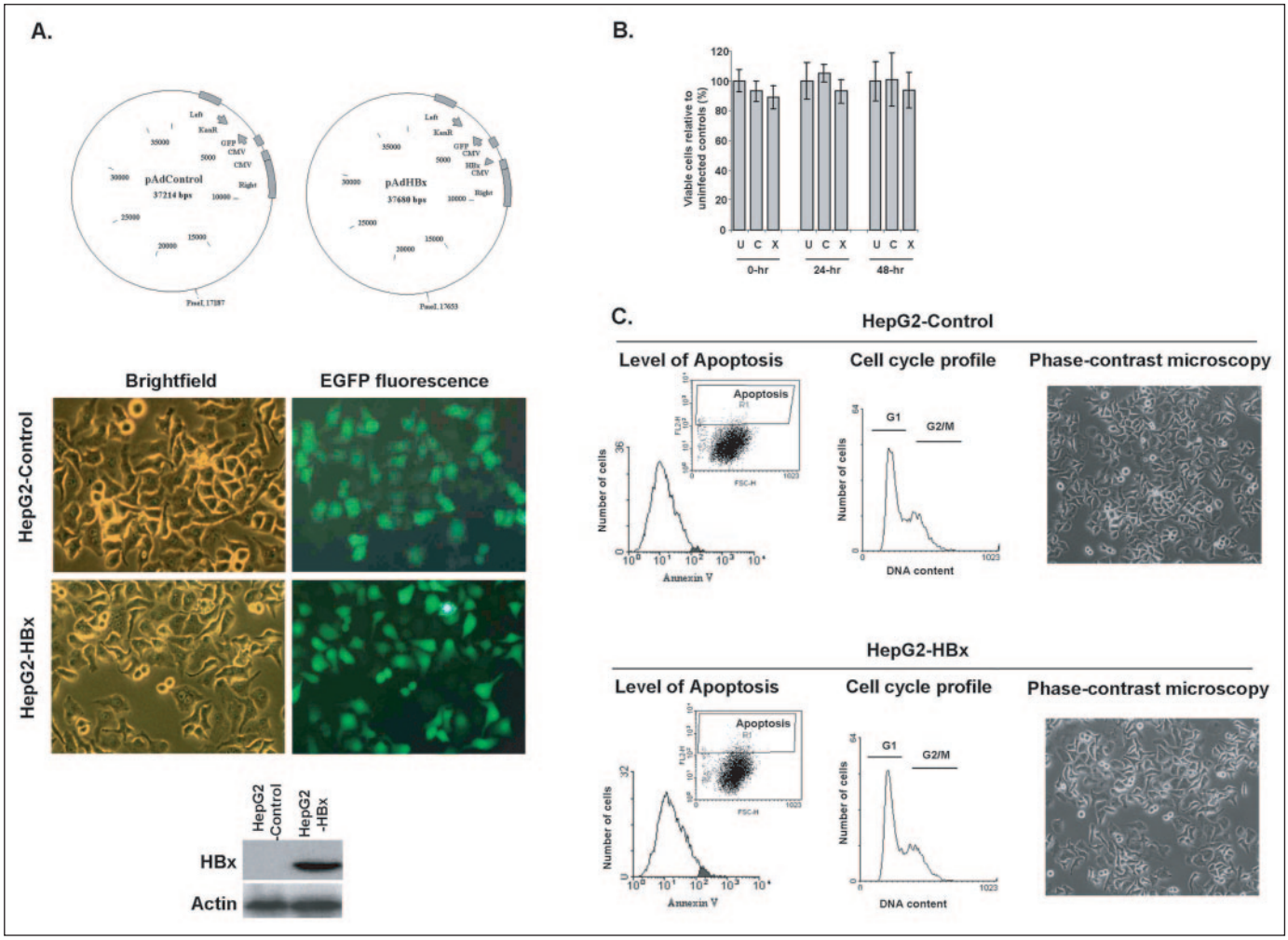

FIGURE 1. **HBx expression does not affect cell morphology, the cell cycle, and apoptosis.** *A*, *upper panels*, shown are schematic diagrams of the pAdControl and pAdHBx constructs used to generate the recombinant adenoviruses. *EGFP*, enhanced green fluorescent protein. *Middle panels*, HepG2 cells were infected with either AdControl or AdHBx at a multiplicity of infection of 5. Cells carrying the recombinant viruses were monitored microscopically by their EGFP fluorescence. *Lower panels*, lysates (30 μg) from HepG2 cells infected with either AdControl (HepG2-Control) or AdHBx (HepG2-HBx) were probed with either anti-HBx or control anti-actin antibody. The blot was exposed to the x-ray film for 30 s. *B*, the viability of AdControl-infected (*C*) or AdHBx-infected (*X*) HepG2 cells relative to uninfected controls (*U*) was determined at various time points after adenovirus infection. *C*, shown are the apoptotic (*left panels*), cell cycle (*middle panels*), and general morphology (*right panels*) profiles of HepG2-Control (*upper panels*) and HepG2-HBx (*lower panels*) cells. The *insets* in the *left panels* show the gated population of apoptotic cells. Similar trends were observed in at least three independent experiments.

of the β-actin housekeeping gene. All reverse transcription-PCRs were performed in triplicate.

Host Cell Reactivation Assay—The β-galactosidase reporter plasmid was damaged with 800 J/m^2 UVC light using a UV cross-linker (UVP, Inc., Upland, CA). Control undamaged β-galactosidase plasmids did not receive UV treatment. Cells were then transfected with the chloramphenicol acetyltransferase (CAT) plasmid and either the damaged or undamaged β-galactosidase reporter plasmid using the Superfect transfection reagent (Qiagen Inc.) according to the manufacturer's protocol. Cell extracts were harvested 48 h after transfection, and assays to detect for β-galactosidase activity and the CAT protein were performed. β-Galactosidase activity was evaluated using chlorophenol red-β-D-galactopyranoside (Roche Applied Science) as substrate to detect β-galactosidase activity in a kinetic assay at 1-min intervals at 570 nm with a SpectraMax Plus^{384} microplate reader (Molecular Devices Corp., Sunnyvale, CA). This β-galactosidase activity was then normalized against CAT protein expression to correct for differences in transfection efficiency. CAT expression was quantitatively measured using a CAT enzyme-linked immunosorbent assay kit (Roche Applied Science). Transfection of the plasmids and the subsequent assays for β-galactosidase activity and CAT expression were performed in control (HepG2-Control) and HBx-infected (HepG2-HBx) HepG2 cells that were either untreated or UV light-irradiated at 8 J/m^2.

RESULTS

HBx Expression Does Not Affect Cell Morphology and Viability, Apoptotic, and Cell Cycle Profiles—A major obstacle in HBx research is the difficulty encountered in obtaining high affinity antibodies to immunodetect the HBx protein (20, 29). Various groups have circumvented this by utilizing either a EGFP-HBx fusion protein (30) or HBx tagged with hemagglutinin at the C terminus (31) for immunoprecipitation or subcellular localization studies. A major disadvantage of these strategies is that, being a small molecule, tagging of HBx with either EGFP or hemagglutinin may alter its solubility or disrupt its normal physiological functions. Here, we report the generation of a specific anti-HBx antibody that is useful for the detection of the HBx protein in Western blots (Fig. 1, *lower panels*), immunoprecipitation (see Fig. 3*D*), and immunocytochemistry (see Fig. 3, *A* and *B*).

We also developed a recombinant AdHBx adenoviral system that has an infection efficiency of >90% as assessed by EGFP fluorescence (Fig. 1*A*, *middle panels*) and that expresses the HBx protein. As shown in Fig.

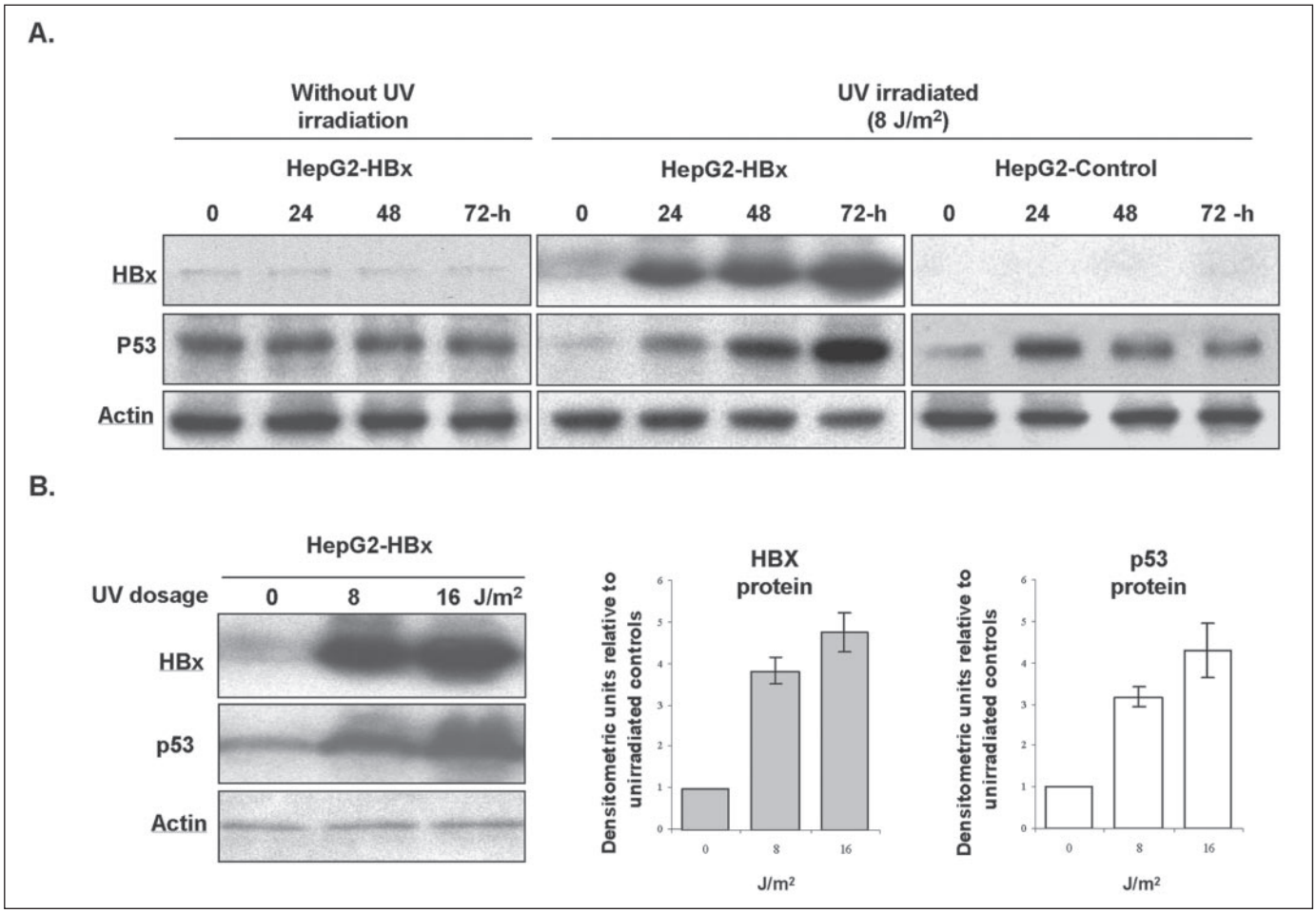

FIGURE 2. **HBx and p53 protein levels in HepG2-Control and HepG2-HBx cells increase after UV irradiation.** *A*, HBx and p53 protein expression in HepG2-Control and HepG2-HBx cells at various time points after UV irradiation (8 J/m^2) was analyzed by Western blot analyses of 10 μg of lysates using anti-HBx (*upper panels*), anti-p53 (*middle panels*), and control anti-actin (*lower panels*) antibodies. *B*, HBx and p53 protein expression in HepG2-Control and HepG2-HBx cells at 24 h after exposure to UV irradiation at 8 and 16 J/m^2 was analyzed by Western blot analyses using anti-HBx (*left upper panel*), anti-p53 (*left middle panel*), and control anti-actin (*left lower panel*) antibodies. Blots probed with anti-HBx antibody were exposed to x-ray film for <5 s. The *middle* and *right panels* show bar diagrams of densitometric quantitation of the Western blots. The results were normalized against actin and are expressed as the means ± S.E. from three independent experiments and are displayed as normalized densitometric units relative to non-UV light-irradiated controls.

1*A* (*bottom panels*), only protein extracts from HepG2 cells infected with AdHBx (HepG2-HBx), but not protein extracts from cells infected with AdControl (HepG2-Control), showed a single distinct band at ~17 kDa, the size of HBx, upon Western blotting.

Previous studies have reported that expression of HBx induces spontaneous apoptotic cell death when expressed in mouse fibroblasts (20), Chang liver cells (18), HepG2 cells (32), and HBx transgenic mouse liver (16). However, we found that expression of HBx was not deleterious to HepG2 cells. Under a phase-contrast microscope, HepG2-HBx cells had a similar morphology and number of doubling mitotic or rounded phase-bright apoptotic cells as the HepG2-Control cells (Fig. 1*C*, *upper right panel*). When cell viability was assessed, there was no statistical difference between the uninfected HepG2 cells and HepG2-Control or HepG2-HBx cells (Fig. 1*B*). Additionally, the apoptotic and cell cycle profiles of HepG2-Control and HepG2-HBx cells were similar (Fig. 1*C*).

p53 and HBx Accumulate in Response to UV Damage—Because our data show that HBx expression did not affect proliferation or induce spontaneous cell death, we hypothesized that the role of HBx as a promoter would be more evident following an initiating event such as DNA damage. DNA damage may precede cellular transformation if DNA repair mechanisms are disrupted (9–11, 33, 34). To evaluate this, we examined the effect of HBx in HepG2 cells exposed to UVC irradiation. Twenty-four hours after infection with AdControl or AdHBx, HepG2-Control or HepG2-HBx cells were exposed to UV damage at a dose of 8 J/m^2. The cells were then harvested at various time points after UV irradiation, and the HBx protein levels in these cells were determined by Western blot analyses. As shown in Fig. 2*A*, *left panels*, in the absence of UV irradiation, only low levels of HBx proteins were observed at the various time points. However, when the cells were UV light-irradiated, the HBx protein was found to accumulate in a time-dependent manner (Fig. 2*A*, *middle panels*). The HBx protein level was also found to increase when the UV dose was increased to 16 J/m^2 (Fig. 2*B*). These results suggest that UV irradiation affects HBx protein levels in a time- as well as dose-dependent manner.

Genotoxic stress (including DNA damage) induces post-transcriptional modification and stabilization of p53, resulting in accumulation of p53 (35). Because p53 is a well known target of HBx (9–11), we evaluated whether the accumulation of p53 in UV light-damaged cells is altered by HBx. As shown in Fig. 2*A*, upon UV irradiation, p53 accumulated in both HepG2-Control and HepG2-HBx cells. However, although p53 protein levels in HepG2-Control cells gradually decreased after an initial peak at 24 h, p53 protein levels continued to increase throughout the experiment in HepG2-HBx cells. Additionally, p53 increased concomitantly with HBx in a dose-dependent manner. Hence, UV irradiation causes an accumulation of both p53 and HBx proteins in HBx-expressing HepG2 cells.

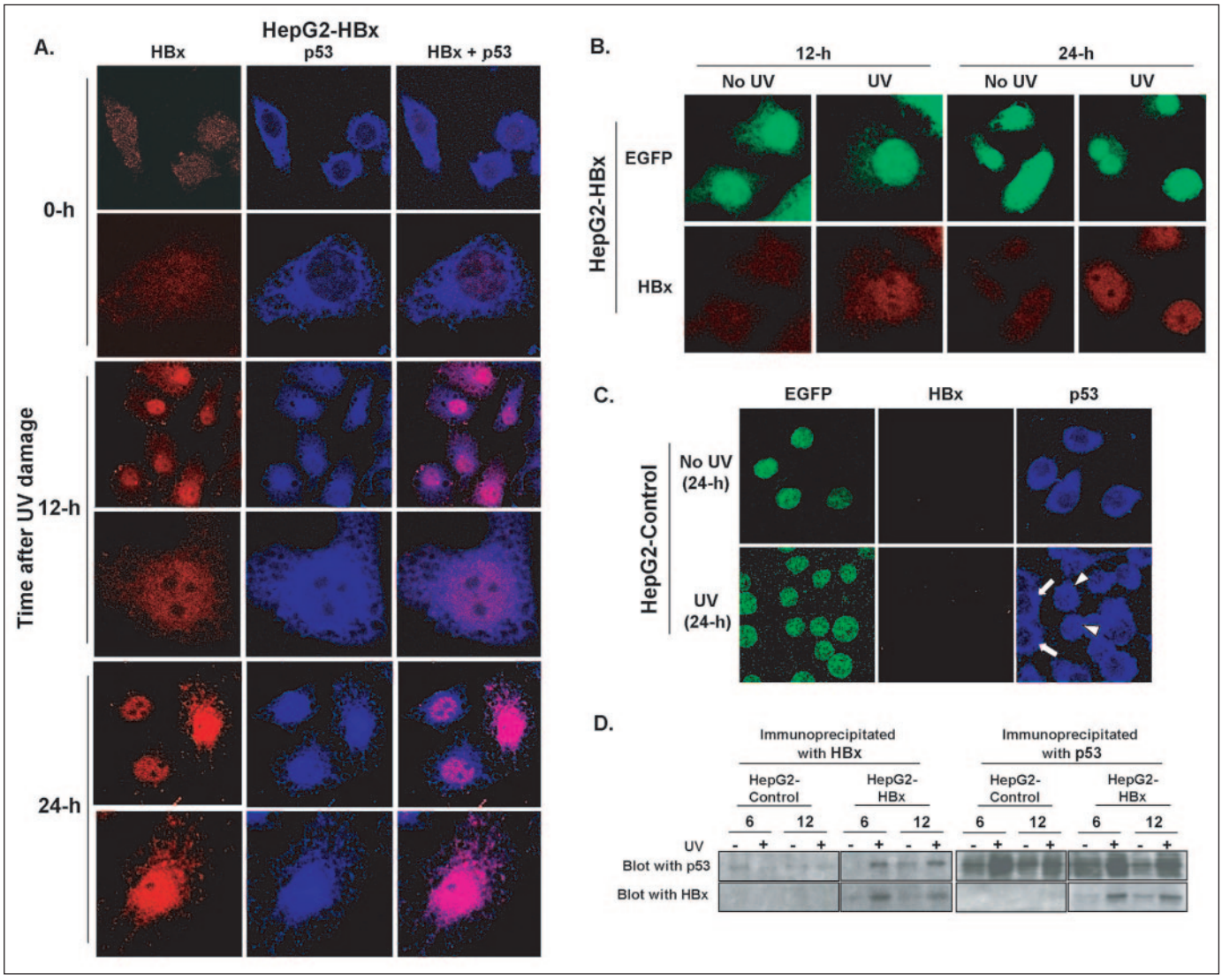

FIGURE 3. **HBx colocalizes and interacts with p53.** *A*, HBx colocalizes with p53. HepG2-HBx cells were grown on coverslips and immunostained with anti-HBx and anti-p53 antibodies. Stained cells were observed under a confocal microscope. The *left panels* show HBx staining; the *middle panels* show p53 staining; and the *right panels* show a pseudo-merge of HBx and p53 staining. The results shown represent a minimum of six fields of vision from three independent experiments. *B*, EGFP fluorescence remains unaffected by UV treatment. Cells grown on coverslips were immunostained with anti-HBx antibody. EGFP and immunostained HBx proteins were observed under a confocal microscope. *C*, less p53 localizes to the nucleus in HepG2-Control cells. HepG2-Control cells were immunostained with anti-HBx and anti-p53 antibodies. EGFP fluorescence and immunostained cells were observed under a confocal microscope. The *left panels* show EGFP fluorescence; the *middle panels* show cells stained with anti-HBx antibody; and the *right panels* display cells stained with anti-p53 antibody. *Arrows* denote cytoplasmic staining of p53, whereas *arrowheads* show nuclear staining of p53. *D*, HBx interacts with p53. HepG2-Control and HepG2-HBx cells were immunoprecipitated with anti-HBx and anti-p53 antibodies and probed with anti-HBx and anti-p53 antibodies on Western blots. The *left panels* show blots immunoprecipitated with HBx, and the *right panels* show blots immunoprecipitated with p53. The *upper panels* show proteins probed with anti-p53 antibody, and the *lower panels* show the same blots probed with anti-HBx antibody.

HBx Colocalizes and Interacts with p53 in the Nucleus upon UV Treatment—The subcellular localization of HBx and p53 in HBx-expressing cells and their biological significance remain unclear. HBx seems to be a nucleocytoplasmic protein (36–38), although it was reported to localize primarily to the cytoplasmic/perinuclear compartment of the cells (24, 25, 31, 39). p53 was reported to bind to HBx (22) and to localize primarily in the cytoplasm (22–24) in HBx-expressing cells. However, HBx was also reported not to colocalize or co-immunoprecipitate with p53 in HBV-infected human liver cells (25).

Because HBx and p53 protein levels were found to increase concomitantly in UV light-treated HepG2-HBx cells (Fig. 2*A*), we assessed whether these two proteins occur in the same subcellular compartment and interact. The immunofluorescence images in Fig. 3*A* (*upper two rows*) show weak HBx staining in both the nuclear and cytoplasmic compartments of untreated HepG2-HBx cells. Upon UV exposure, there was an increase in HBx staining primarily in the nucleus (Fig. 3*A*, *lower four rows*), suggesting nuclear accumulation of HBx in these cells. This increase in HBx staining in UV light-damaged cells confirms our earlier immunoblot observation of increased HBx protein levels in UV light-treated HepG2-HBx cells (Fig. 2).

It is possible that the increased HBx protein levels are due to an increase in promoter activity in response to UV. However, this is unlikely. In our adenoviral construct, both the HBx gene and the EGFP gene (transfection efficiency control) were driven by cytomegalovirus (CMV) promoters (Fig. 1*A*). As shown in Fig. 3 (*B* and *C*), EGFP staining was similar in both control and UV light-treated cells, suggesting that UV treatment does not affect CMV promoter activity. Hence, our data suggest that the observed increase in HBx levels shown in Figs. 2*A* and 3*A* may be due to protein stabilization and not increased transcriptional activity in response to UV treatment.

Interestingly, upon UV treatment, cytoplasmic p53 was found to be translocated into the nucleus of a greater number of HepG2-HBx com-

pared with HepG2-Control cells. In untreated HepG2-Control cells (Fig. 3*C*, *upper panels*) and HepG2-HBx cells (Fig. 3*A*, *upper two rows*), p53 was localized primarily in the cytoplasm. However, when these cells were irradiated with 8 J/m^2 UV light, p53 staining in ~10% of the HepG2-Control cells (Fig. 3*C*, *lower panels*) and ~80% of the HepG2-HBx cells (Fig. 3*A*, *lower four rows*) was in the nucleus. The percentage of p53 staining in the nucleus was determined by counting the number of nuclear stained p53 cells *versus* the number of total cells from a minimum of six random fields from three independent experiments. Significantly, both p53 and HBx were found to colocalize in the nucleus upon UV irradiation (Fig. 3*A*, *lower four rows*).

To evaluate whether HBx interacts with p53, cell extracts from untreated or UV light-treated HepG2-Control or HepG2-HBx cells were immunoprecipitated with either anti-HBx or anti-p53 antibody and then probed with either of the two antibodies. Fig. 3*D* shows that the HBx protein was not detected in the anti-HBx or anti-p53 antibody-immunoprecipitated fraction of either untreated or UV light-treated HepG2-Control cells. In untreated HepG2-HBx cells, a low level of coprecipitated p53 protein was detected in the anti-HBx immunoprecipitate due to the presence of low basal levels of HBx (Fig. 2). However, upon UV irradiation, the p53 protein was detected in the anti-HBx antibody-immunoprecipitated fraction, and the HBx protein was detected in the anti-p53 antibody-immunoprecipitated fraction of the HepG2-HBx cell extracts (Fig. 3*D*). Together with the immunofluorescence observations, these findings suggest that p53 associates with HBx and that both these proteins accumulate in the nucleus upon UV damage.

HBx-p53 Interaction Does Not Abrogate p53-mediated Transcriptional Activation—Previous reports have shown that p53 acts as a transcriptional regulator of *MDM2*, p21, and *bax*, among many others (40, 41). Our observation that HBx colocalized and associated with p53 in the nucleus suggested that HBx may interfere with p53 function in the nucleus, resulting in p53 target genes not being transactivated. To address whether HBx interaction with p53 inhibits p53 transactivation functions, we assessed the expression of three p53 target genes involved in the cell cycle and apoptosis using comparative real-time reverse transcription-PCR. As shown in Fig. 4, HBx interaction with p53 did not abrogate or significantly alter the transactivation of *MDM2* by p53. The ability of p53 to transactivate p21 and *bax*/*bcl-2* was altered (but not abrogated) by HBx-p53 interaction.

In HepG2-Control cells, p21 gene expression increased to a maximum of 4.5-fold of that in untreated cells at 6 h after UV treatment and was maintained at approximately that maximum level throughout the experiment (Fig. 4*A*). However, in HepG2-HBx cells, p21 gene expression increased to ~7-fold of that in untreated cells at 12 and 24 h after UV treatment, which is nearly 2-fold greater than in HepG2-Control cells at 12 and 24 h after UV treatment (Fig. 4*A*). This greater p21 gene expression in HepG2-HBx cells compared with HepG2-Control cells at 12 and 24 h after UV exposure is suggestive of increased cell cycle arrest of HepG2-HBx cells (42). Forty-eight hours after UV exposure, p21 gene expression in HepG2-Control cells was maintained at ~5.5-fold of that in untreated cells, whereas its expression in HepG2-HBx cells was significantly reduced to ~3-fold of that in untreated cells. Because p21 has been reported to be an inhibitor of apoptosis (43), our observations suggest that HepG2-HBx cells may be directed toward the apoptotic pathway as evident by a decrease in p21 gene expression.

The profile of the expression ratios of pro-apoptotic *bax versus* anti-apoptotic *bcl-2* was different between HepG2-Control and HepG2-HBx cells (Fig. 4*C*). Although the *bax*/*bcl-2* ratio in HepG2-Control cells gradually increased to a maximum of nearly 3-fold greater that that in untreated cells at 24 h before decreasing to slightly <1.5-fold of that in

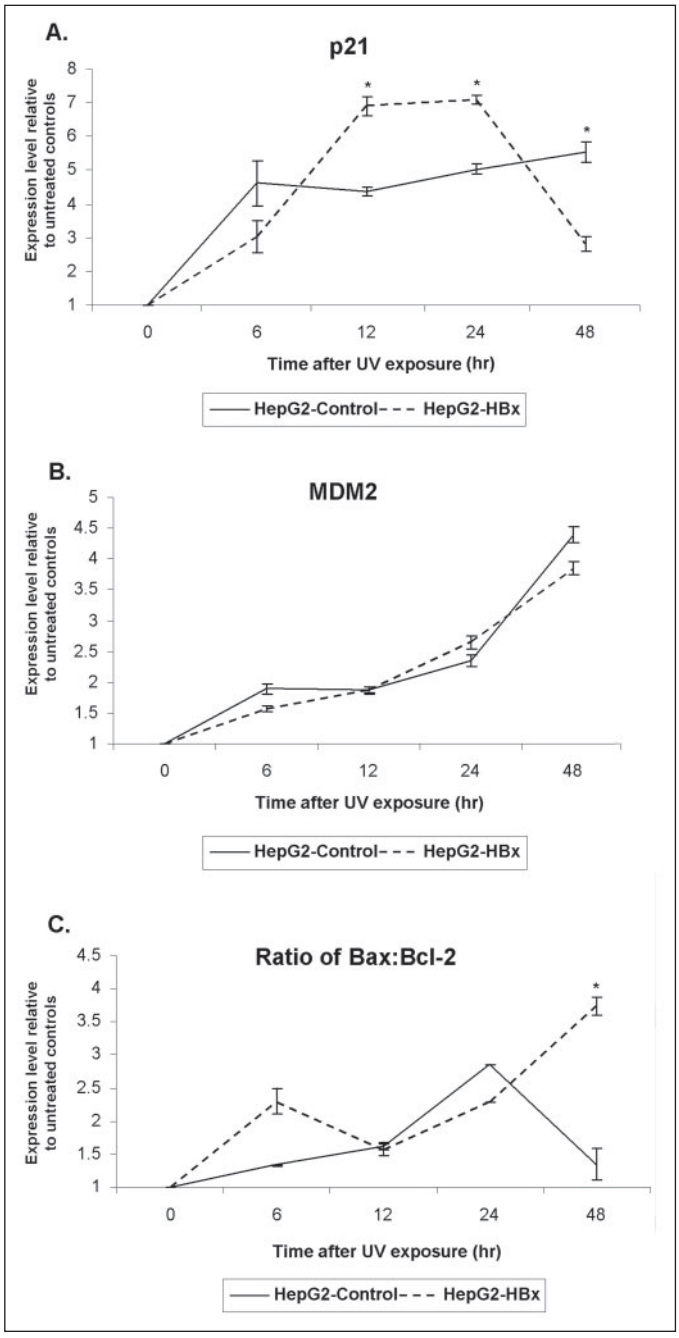

FIGURE 4. **Expression of p53-responsive genes is not abrogated by HBx.** At the indicated time points after UV exposure, the expression of various p53-responsive genes was determined using real-time reverse transcription-PCR. *A*, p21 gene; *B*, *MDM2*; *C*, *bax/bcl-2* expression ratios. The results are expressed as the means ± S.E. from three independent experiments and are displayed as expression levels relative to untreated control samples. *, significant difference at $p < 0.05$ between HepG2-Control and HepG2-HBx cells at the particular time points indicated.

untreated cells at 48 h, the *bax*/*bcl-2* ratio in HepG2-HBx cells increased to nearly 2.5-fold greater than that in untreated cells at 6 h and then decreased to slightly >1.5-fold of that in untreated cells at 12 h before increasing again to ~4-fold at 48 h. These results suggest that, during UV damage, the initial response in HepG2-Control cells is a slight increase in apoptosis as shown by an ~3-fold increase in *bax*/*bcl-2* levels at 24-h. Forty-eight hours after UV treatment, fewer cells are directed toward the apoptotic pathway, with the *bax*/*bcl-2* ratio decreasing to <1.5-fold, suggesting that the cells may have repaired their damaged DNA. However, HepG2-HBx cells are directed toward the apoptotic pathway more rapidly as shown by an ~2.5-fold increase

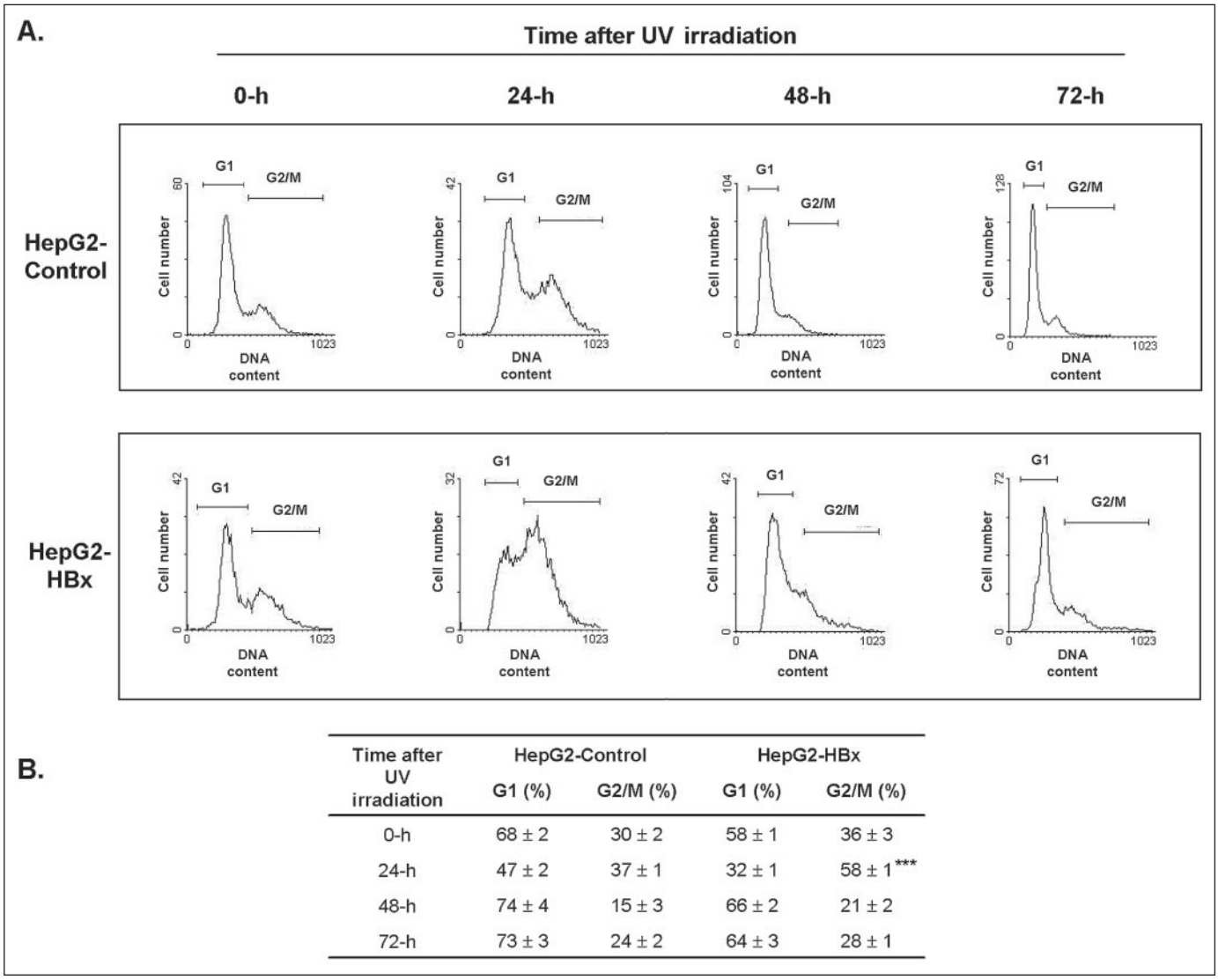

B.

Time after UV irradiation	HepG2-Control		HepG2-HBx	
	G1 (%)	G2/M (%)	G1 (%)	G2/M (%)
0-h	68 ± 2	30 ± 2	58 ± 1	36 ± 3
24-h	47 ± 2	37 ± 1	32 ± 1	58 ± 1***
48-h	74 ± 4	15 ± 3	66 ± 2	21 ± 2
72-h	73 ± 3	24 ± 2	64 ± 3	28 ± 1

FIGURE 5. **Increased G_2/M cell cycle arrest of HepG2-HBx cells following UV treatment.** *A*, HepG2-Control and HepG2-HBx cells were exposed to UV irradiation for the indicated periods and stained with propidium iodide. Cell cycle profiles were then assessed by flow cytometry. The profiles displayed are representative of at least three independent experiments. *B*, the means ± S.E. from these three experiments are presented. ***, statistically significant difference at $p < 0.001$ in the percentage of HepG2-Control and HepG2-HBx cells in G_2/M phase.

in the *bax*/*bcl-2* ratio at 6 h after UV treatment. This is likely followed by cell cycle arrest of these HepG2-HBx cells in an attempt to repair the damage at 12 h as evident by an increase in p21 gene expression and a decrease in the *bax*/*bcl-2* ratio at 24 h. We hypothesized that HepG2-HBx cells are more predisposed to apoptosis at 48 h after UV treatment as evident by the decrease in p21 gene expression (Fig. 4*A*) and the increase in the *bax*/*bcl-2* ratio (Fig. 4*C*) because these cells were unable to efficiently repair DNA damage.

Collectively, these data suggest that the transcriptional capability of p53 is altered (but not abrogated) by its interaction with HBx. This altered function of p53 affects the cell cycle and apoptotic profiles of HBx-expressing cells and suggests that the DNA repair mechanism of these cells may also be affected.

HBx Sensitizes HepG2 Cells to Cell Cycle Arrest and Apoptosis following UV Damage—The alteration of the expression of p53-responsive genes (Fig. 4) suggests that HBx-expressing cells may have altered cell cycle or apoptotic profiles. Flow cytometry was employed to directly assess the effect of HBx expression on cell cycle progression after UV damage. Fig. 5*A* shows representative cell cycle profiles of HepG2-Control and HepG2-HBx cells at various time points after UV irradiation. Results from three independent experiments showing the percentage of cells in the G_1 and G_2/M phases of the cell cycle are presented in Fig. 5*B*.

As shown in Fig. 5, at 24 h after UV damage, there was a slight increase in the percentage of HepG2-Control cells in G_2/M phase. This is consistent with a previous study showing that UV exposure of cells can lead to G_2/M arrest (44). Arresting cells at the G_2/M transition was found to prevent the premature segregation of damaged DNA before repair takes place (45, 46). In contrast, significantly greater G_2/M arrest was observed in HepG2-HBx cells compared with HepG2-Control cells at 24 h after UV treatment ($p < 0.001$) (Fig. 5). This increased G_2/M arrest correlated with increased p21 expression at 12–24 h after UV irradiation (Fig. 4). Forty-eight hours after UV treatment, the cell cycle profiles of both HepG2-Control and HepG2-HBx cells returned to those of the pretreatment stage (Fig. 5).

Three approaches were employed to assess the apoptotic profiles of HepG2-Control and HepG2-HBx cells after UV treatment. By phase-contrast microscopy (Fig. 6*C*), we found that, in the absence of UV light, the morphology of HepG2-Control and HepG2-HBx cells was similar. However, after UV irradiation, there were more rounded floating phase-bright apoptotic cells in HBx-expressing cells compared with control

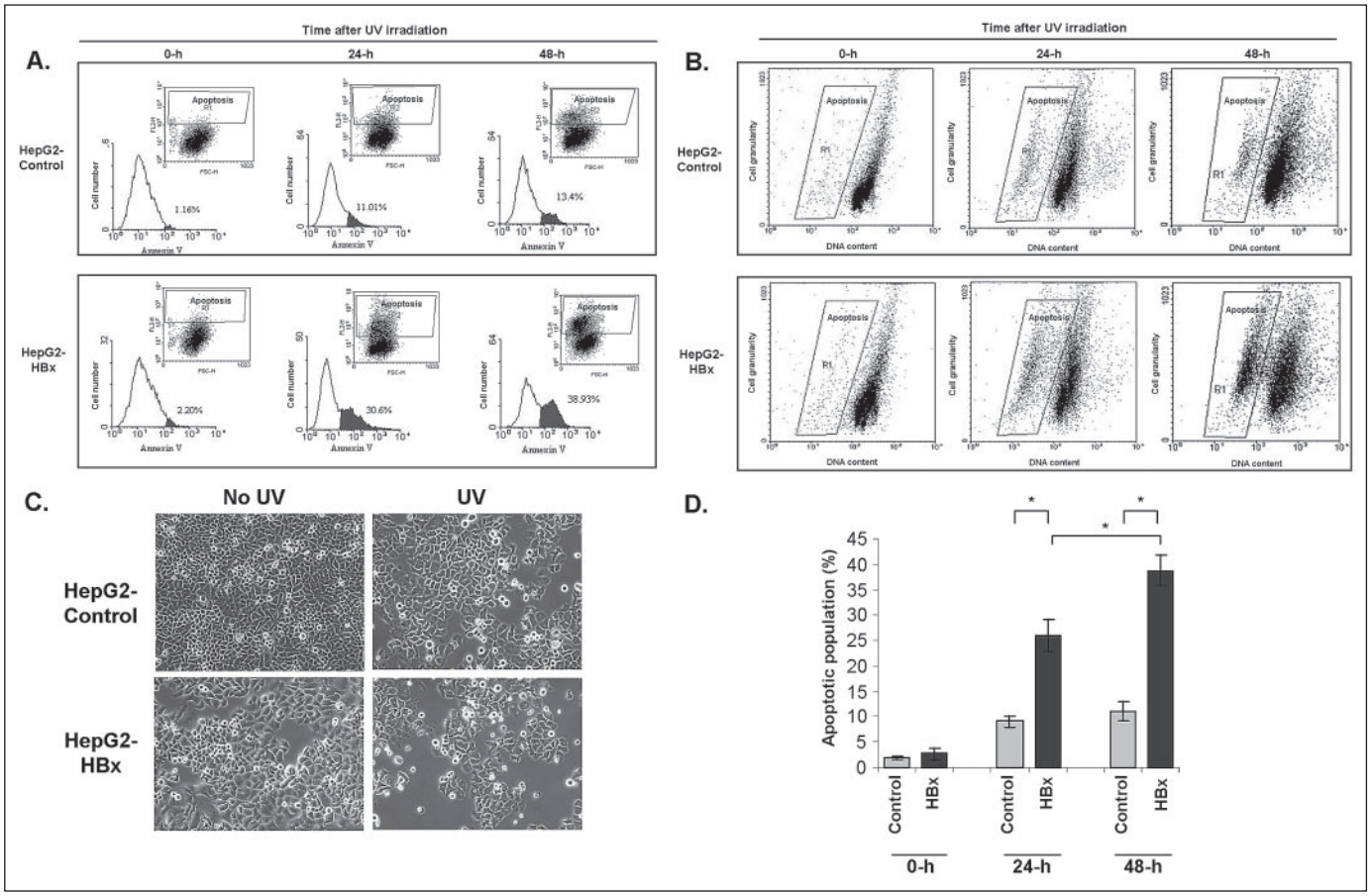

FIGURE 6. **Increased apoptosis of HepG2-HBx cells following UV damage.** *A*, UV light-exposed HepG2-Control and HepG2-HBx cells were stained with phycoerythrin-conjugated annexin V to detect phosphatidylserine externalization in apoptotic cells and were analyzed by flow cytometry. The *insets* show the gated population of apoptotic cells. *B*, apoptotic populations of HepG2-Control and HepG2-HBx cells exposed to UV irradiation were also assessed based on their propidium iodide staining and light scattering properties. The *x axes* show DNA content (propidium iodide staining), and the *y axes* show cell granularity (side scatter). The *gated areas* represent apoptotic cells. Apoptotic cells characteristically showed an increase in cell granularity and a lower DNA content. *C*, phase-contrast images are shown of HepG2-Control and HepG2-HBx cells. *D*, shown are the means ± S.E. of the percentage of apoptotic HepG2-Control and HepG2-HBx cells exposed to UV irradiation for the indicated periods of time obtained from six independent phycoerythrin-conjugated annexin V and propidium iodide staining assays. *, statistically significant difference at $p < 0.05$ in the percentage of apoptotic HepG2-Control and HepG2-HBx cells at the times indicated as well as HepG2-HBx cells between 24 and 48 h after UV treatment.

cells. Apoptosis of these cells was also evaluated by flow cytometry of annexin V-stained cells (Fig. 6*A*) as well as propidium iodide-stained cells analyzed by their propidium iodide fluorescence and side scatter plots (Fig. 6*B*). The means ± S.E. of the percentage of apoptotic HepG2-Control/HepG2-HBx cells before and after UV treatment from results obtained with a combination of three independent experiments with annexin V-stained cells and three independent experiments with propidium iodide-stained cells are presented in Fig. 6*D*. As shown in Fig. 6, there was a modest increase in the apoptosis of HepG2-Control cells at 24 h (~10%) and 48 h (~12%) after UV treatment. This is consistent with a previous report of a similar modest increase in apoptosis of primary hepatocytes exposed to a similar dosage of UV light (47). In contrast, HepG2-HBx cells were found to be more sensitive to UV damage and exhibited a significantly greater percentage of apoptotic cells compared with HepG2-Control cells ($p < 0.05$) at 24 and 48 h after UV exposure (Fig. 6*D*).

The initial increased G_2/M arrest of HepG2-HBx cells at 24 h after UV treatment and the sustained increased apoptosis of these cells at 24 and 48 h after UV exposure suggest that the repair mechanism in HepG2-HBx cells may be impaired, hence predisposing these cells toward the apoptotic pathway. We thus proceeded to examine whether UV light-irradiated HepG2-HBx cells are able to repair UV light-damaged DNA as efficiently as HepG2-Control cells.

HBx Reduces the Ability of UV Light-damaged Cells to Repair Damaged DNA—Hepatocytes do not readily succumb to apoptosis in response to DNA damage (47), suggesting that the induction of a repair mechanism is favored over induction of cell death (48). UV irradiation causes DNA damage through helix distortions, and the damage is repaired by the nucleotide excision repair (NER) pathway (49). To assess the possible effect of HBx on the NER pathway, we compared the abilities of HepG2-Control and HepG2-HBx cells to repair an *in vitro* damaged β-galactosidase reporter plasmid using the host cell reactivation assay, which reflects the NER of damaged DNA (50). UV light-irradiated or non-irradiated cells were transfected with either an undamaged or a UV light-damaged β-galactosidase reporter plasmid. A CAT plasmid was cotransfected to monitor transfection efficiency. As shown in Fig. 7*A*, untreated control or HBx-expressing cells transfected with either the undamaged or UV light-damaged reporter plasmid displayed similar β-galactosidase reporter activity, indicating that HBx expression does not affect the NER machinery when there is no UV exposure.

However, when these cells were UV light-irradiated at 8 J/m^2, the ability of the HepG2-HBx cells to repair the damaged DNA was significantly different compared with HepG2-Control cells ($p < 0.05$) (Fig. 7*B*). Although irradiated control cells displayed similar β-galactosidase activity compared with non-irradiated control cells, irradiated HBx-expressing cells showed significantly reduced β-galactosidase activity compared with non-irradiated HBx-expressing cells. This result suggests that HBx-expressing cells exposed to UV irradiation are unable to repair damaged DNA as efficiently as control cells.

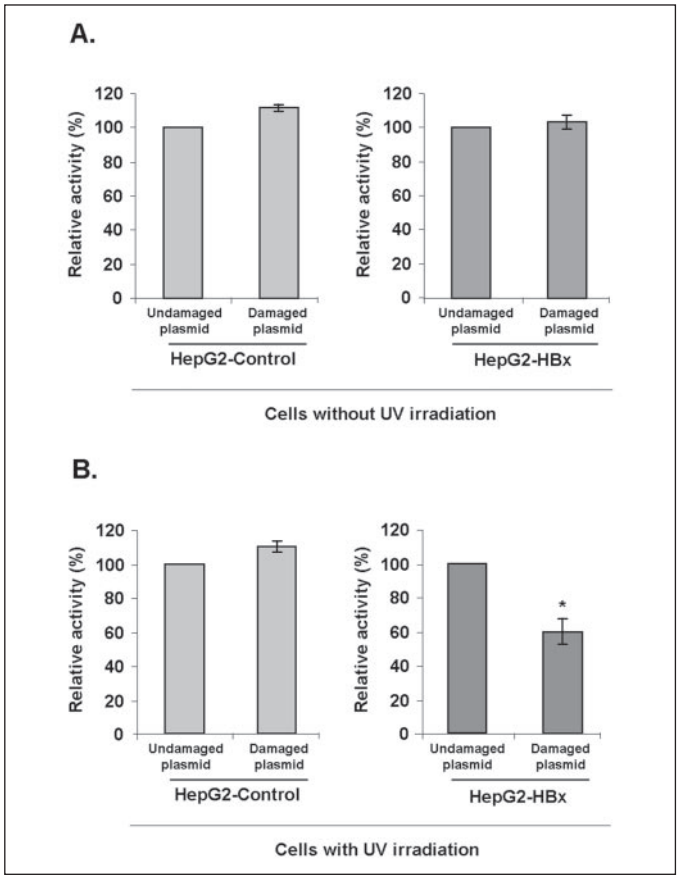

FIGURE 7. **UV light-exposed HepG2-HBx cells have a reduced DNA repair capability.** HepG2-Control and HepG2-HBx cells were cotransfected with either an undamaged or a damaged β-galactosidase reporter plasmid as well as a CAT plasmid to normalize for differences in transfection efficiency. *Relative activity (%)* represents the normalized β-galactosidase activity of untreated (*A*) or UV light-irradiated (*B*) cells carrying either plasmid relative to the normalized β-galactosidase activity of cells carrying the undamaged plasmid. The results are the means ± S.E. from three independent experiments. *, statistically significant difference at $p < 0.05$ in the relative β-galactosidase activity of UV light-irradiated HepG2-HBx cells carrying undamaged and damaged plasmids.

DISCUSSION

Numerous studies have been performed to elucidate the role of the virally encoded HBx protein in promoting HCC. However, thus far, most published reports provide only snapshots of its pleiotropic functions as a promoter in carcinogenesis, with insufficient evidence directly implicating an initiating factor in affecting HBx function in the cell. In this study, we present data to address the effects of HBx expression in cells exposed to UV light-induced DNA damage as an initiating factor.

In the absence of UV damage, cells expressing HBx were found to be similar to control cells in their morphology, cell cycle, and apoptotic profiles (Fig. 1). Untreated HBx-expressing cells were also able to repair damaged DNA as efficiently as control cells (Fig. 7). Similar observations were reported for untreated HBx-expressing cells and transgenic mice (8, 17, 48, 51). This observation is consistent with the notion that, in the absence of an initiating factor, the benign nature of HBx will favor HBV survival during the early stages of infection because the virus titer during this period may be insufficient for propagation (49). Nonetheless, untreated HBx-expressing cells have also been reported to exhibit increased proliferation and apoptosis as well as altered cell cycle profiles and ability to repair damaged DNA (3, 6, 7, 20, 30, 50, 52).

Upon DNA damage, normal hepatocytes are usually directed toward the cellular repair response pathway rather than the apoptotic pathway (47, 48). In contrast, increased apoptosis has been observed in the livers of patients with chronic HBV infection (53). In this study, HBx-expressing cells were found to exhibit increased sensitivity to G_2/M arrest as well as apoptosis after UV irradiation (Figs. 5 and 6). This increased G_2/M arrest and apoptosis correlated with increased levels of HBx protein (Fig. 2) in the nucleus (Fig. 3*A*) in UV light-irradiated HBx-expressing cells. The increased HBx protein expression is likely due to increased HBx protein stabilization rather than increased transcriptional activity in UV light-irradiated cells. Similar levels of EGFP expression were observed in the presence and absence of UV irradiation (Fig. 3, *B* and *C*), suggesting that UV treatment does not affect the CMV promoter. Because both the HBx and EGFP proteins were driven by similar CMV promoters in our construct, it is thus unlikely that UV irradiation affected the transcriptional activity of HBx. The HBx protein has been reported to have a short half-life (~30 min) and is rapidly degraded by the proteasome pathway (54–56). Our observation of increased HBx protein accumulation in a time- and dose-dependent manner upon UV treatment is suggestive of the stabilization of the HBx protein upon UV irradiation. This is consistent with reports of the interaction between HBx and damaged DNA-binding (DDB) proteins, which results in the stabilization of HBx and the prevention of the proteasomal degradation of HBx when it is bound to UV light-induced DDB1 (57, 58). Additionally, DDB2 was found to associate with HBx and to enhance the nuclear accumulation of HBx (59). The UV-damaged DNA-binding protein (UV-DDB) complex formed by DDB1 and DDB2 exhibits high binding affinity for UV light-damaged DNA and has been implicated in global genomic repair (60–62). The binding of HBx to UV-DDB has been reported to decrease the capacity of the cell to correct lesions in the genome (6, 63). HBx was also found to associate with XPB and XPD, components of the transcription factor IIH complex involved in the NER pathway, and to decrease DNA repair efficiency (50, 64). Additionally, the interaction of HBx and DDB1 in the nucleus has been reported to promote cell death (65). This is consistent with our current observation that, upon UV treatment, there was increased accumulation of HBx in the nucleus (Fig. 3), a reduced capacity to repair damaged DNA (Fig. 7), and increased apoptosis (Fig. 6) in HBx-expressing cells.

p53 has been reported to play a role in the stress response pathway to decide the fate of the stressed cells toward either survival, involving cell cycle arrest, which will facilitate the repair of the damaged DNA, or death, involving either apoptosis or necrosis (12). UV irradiation, which causes DNA damage, was found to elicit the p53-dependent stress response by activating p53 through the stabilization of the protein in the nucleus (12). Consistent with this, we also observed an increase in p53 protein levels in both control and HBx-expressing cells after UV treatment (Fig. 2), likely as a stress response to UV damage. In control cells, p53 accumulated in the nucleus (Fig. 3*C*), and the levels peaked at 24 h after UV treatment and then decreased thereafter (Fig. 2*A*, *second row*, *right panel*). This correlated with an increase in G_2/M arrest (Fig. 5*A*) and a modest increase in apoptosis at 24 h after UV treatment (Fig. 6) and the ability to repair UV light-damaged DNA (Fig. 7). The cell cycle profile returned to normal thereafter (Fig. 5*A*), and no further increase in apoptosis was observed (Fig. 6). These results suggest that normal cells respond to UV stress by stabilizing p53 levels in the nucleus, resulting in cell cycle arrest, which provides time for repair of the damaged DNA before cell division. After the damaged DNA is repaired, the cell cycle returns to normal. A small fraction of the cells that cannot be repaired are directed toward the apoptotic pathway (Fig. 8).

Interestingly, upon UV irradiation, the p53 protein in HBx-expressing cells accumulated in a time-dependent manner (Fig. 2*A*, *second row*, *middle panel*), which correlated with the time-dependent increase in the HBx protein (*first row*, *middle panel*) in the nucleus of the cells (Fig. 3*A*). Greater nuclear accumulation of p53 was observed in HBx-expressing cells compared with control cells (Fig. 3). Colocalization (Fig.

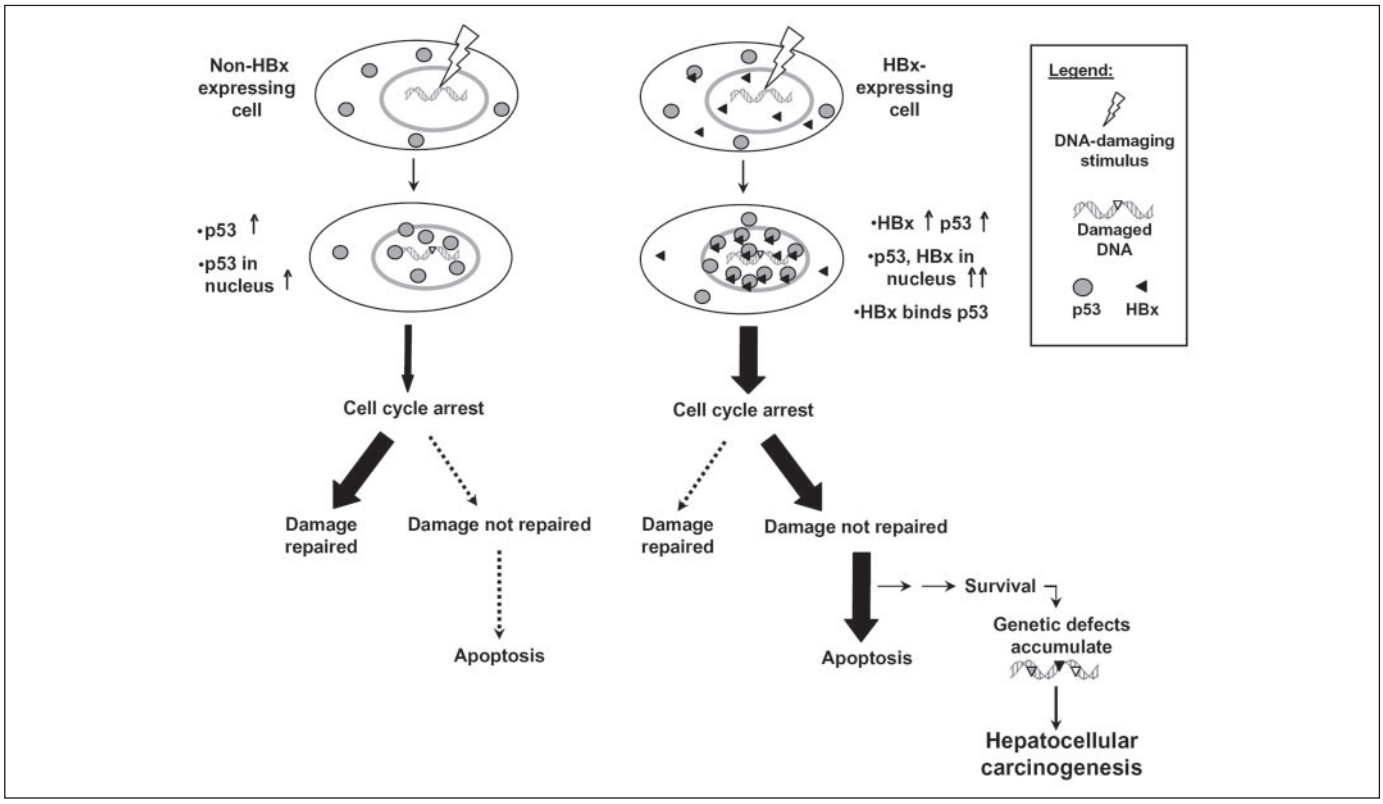

FIGURE 8. **Hypothetical model of the role of HBx in hepatocarcinogenesis via its modulation of cellular response to DNA damage.**

3*A*) and interaction (Fig. 3*D*) of the p53 and HBx proteins were observed. The interaction of HBx with p53 could have further stabilized the p53 protein probably through interfering with the interaction of p53 with MDM2 (66). p53 and MDM2 are components of an autoregulatory feedback loop whereby p53 transcriptionally activates MDM2, which, in turn, inhibits p53 transcriptional functions (67, 68) as well as induces the nuclear export and degradation of p53 (69, 70). Hence, although the expression of MDM2 mRNA is similar in control and HBx-expressing cells (Fig. 4*B*), the association of HBx and p53 may have prevented the interaction of p53 with MDM2 and caused greater nuclear accumulation of p53 in HBx-expressing cells. Additionally, we found that HBx-p53 interaction also resulted in modulation of the expression of some of the p53 target genes, including p21 and *bax*/*bcl-2* (Fig. 4). Significantly increased G_2/M arrest (Fig. 5) and apoptosis (Fig. 6) were found in HBx-expressing cells compared with control cells at 24 h after UV treatment. Unlike in control cells, in HBx-expressing cells exposed to UV irradiation, although the cell cycle profile returned to normal thereafter (Fig. 5), the percentage of apoptotic cells continued to increase significantly (Fig. 6). Additionally, HBx-expressing cells exposed to UV irradiation were found to exhibit a reduced ability to repair UV light-damaged DNA compared with control cells (Fig. 7). Taken together, these data suggest that, in HBx-expressing cells, UV treatment likely stabilizes and increases the levels of both HBx and p53 proteins (Fig. 8). These two proteins interact and colocalize to the nucleus, where HBx further stabilizes the p53 protein and modulates p53 function as a transactivator, altering the expression of some of the p53 target genes. HBx has been reported to bind to the C terminus of p53 (19), a region implicated in the binding of p53 to XPB and XPD (71), which are important components of the NER pathway. Hence, the interaction of HBx with p53 may also affect cellular repair mechanisms. This is evident from our observation that HBx-expressing cells exposed to UV irradiation did not repair UV light-damaged DNA as efficiently as control cells (Fig. 7) as well as a report that the HBx protein inhibits DNA repair in a p53-dependent manner (48). The initial increased cell cycle arrest and apoptosis at 24 h after UV treatment in HBx-expressing cells compared with control cells suggests that HBx expression sensitizes cells toward greater G_2/M arrest and apoptosis. The gradual return of the cell cycle (but not apoptotic) profiles of HBx-expressing cells to the pre-UV state and the reduced ability of these cells to repair damaged DNA suggest that these arrested HBx-expressing cells whose DNA is not repaired are being directed toward the apoptotic pathway.

Curiously, our data seem to differ from previous reports implicating the HBx-p53 complex in abrogating apoptosis (19, 23) and inhibiting p53-mediated transactivation (19) in the cytoplasm. A possible explanation for this seeming discrepancy could be due to differences in the experimental setup. Although we examined endogenous p53 in HBx-expressing cells in response to UV light-induced damage, the previous reports examined artificial overexpression of p53 and HBx by microinjection. Hence, the relevance of their results remains uncertain.

In summary, we propose a hypothetical model of the role of HBx in hepatocarcinogenesis in response to DNA damage (Fig. 8). Being a protein with pleiotropic functions, HBx may modulate the cellular response to DNA damage in two ways. First, it may affect the ability of the cell to repair damaged DNA (Fig. 7). In the presence of UV damage, the HBx protein is stabilized and accumulates in the nucleus (Figs. 2 and 3) probably by interacting with DDB proteins (57–59). The interaction of HBx with these proteins may affect the ability of these proteins to correct lesions in the genome (6, 63). HBx may also associate with XPB/XPD either directly (50, 64) or indirectly through binding to p53 (19) to interfere with DNA repair (50). These cells with a reduced ability to repair damaged DNA are thus more susceptible to mutations and malignancy as demonstrated in NER-defective inherited diseases, *e.g.* xeroderma pigmentosum (33, 34). Hence, HBx may play a role in the carcinogenesis process by affecting the ability of cells to repair damaged DNA, resulting in increased genetic lesions and predisposing a chronic HBV-infected individual to cancer.

Second, HBx may affect the cellular response to DNA damage by directing these cells toward the apoptotic (Fig. 6) rather than repair (Fig. 7) pathway. HBx was found to interact with p53 (Fig. 3*D*), stabilizing the p53 protein (Fig. 2) in the nucleus (Fig. 3*A*) and affecting its functions (Fig. 4), including perhaps induction of apoptosis because p53 is known to activate apoptosis (72, 73). Hence, HBx direction of cells toward the apoptotic pathway may be a strategy that HBV employs to facilitate its own propagation during the late stages of infection. Apoptotic hepatocytes undergo blebbing and form membrane-bound apoptotic bodies carrying the viruses that are engulfed by neighboring cells without evoking an immune response. This will contribute to the spread of the virus and hence ensure its persistence (74, 75). Additionally, the role of HBx in sensitizing cells to apoptosis coupled with impairing the ability of cells to repair damaged DNA could favor the carcinogenesis process. Induction of apoptosis and impairment of cellular repair machinery may present a selective advantage for the clonal propagation of apoptosis-resistant mutant preneoplastic cells, which can give rise to HCC.

Acknowledgment—We thank Joo Yee Ng for invaluable technical assistance.

REFERENCES

1. Beasley, R. P. (1988) *Cancer* **61,** 1942–1956
2. Kim, C. M., Koike, K., Saito, I., Miyamura, T., and Jay, G. (1991) *Nature* **351,** 317–320
3. Koike, K., Moriya, K., Yotsuyanagi, H., Iino, S., and Kurokawa, K. (1994) *J. Clin. Investig.* **94,** 44–49
4. Slagle, B. L., Lee, T. H., Medina, D., Finegold, M. J., and Butel, J. S. (1996) *Mol. Carcinog.* **15,** 261–269
5. Terradillos, O., Billet, O., Renard, C. A., Levy, R., Molina, T., Briand, P., and Buendia, M. A. (1997) *Oncogene* **14,** 395–404
6. Becker, S. A., Lee, T. H., Butel, J. S., and Slagle, B. L. (1998) *J. Virol.* **72,** 266–272
7. Groisman, I. J., Koshy, R., Henkler, F., Groopman, J. D., and Alaoui-Jamali, M. A. (1999) *Carcinogenesis* **20,** 479–483
8. Madden, C. R., Finegold, M. J., and Slagle, B. L. (2000) *J. Virol.* **74,** 5266–5272
9. Feitelson, M. A., Zhu, M., Duan, L. X., and London, W. T. (1993) *Oncogene* **8,** 1109–1117
10. Wang, X. W., Forrester, K., Yeh, H., Feitelson, M. A., Gu, J. R., and Harris, C. C. (1994) *Proc. Natl. Acad. Sci. U. S. A.* **91,** 2230–2234
11. Takada, S., Tsuchida, N., Kobayashi, M., and Koike, K. (1995) *J. Cancer Res. Clin. Oncol.* **121,** 593–601
12. Schwartz, D., and Rotter, V. (1998) *Semin. Cancer Biol.* **8,** 325–336
13. Su, F., and Schneider, R. J. (1996) *J. Virol.* **70,** 4558–4566
14. Gottlob, K., Fulco, M., Levrero, M., and Graessmann, A. (1998) *J. Biol. Chem.* **273,** 33347–33353
15. Shih, W. L., Kuo, M. L., Chuang, S. E., Cheng, A. L., and Doong, S. L. (2000) *J. Biol. Chem.* **275,** 25858–25864
16. Koike, K., Moriya, K., Yotsuyanagi, H., Shintani, Y., Fujie, H., Tsutsumi, T., and Kimura, S. (1998) *Cancer Lett.* **134,** 181–186
17. Bergametti, F., Prigent, S., Luber, B., Benoit, A., Tiollais, P., Sarasin, A., and Transy, C. (1999) *Oncogene* **18,** 2860–2871
18. Sirma, H., Giannini, C., Poussin, K., Paterlini, P., Kremsdorf, D., and Brechot, C. (1999) *Oncogene* **18,** 4848–4859
19. Wang, X. W., Gibson, M. K., Vermeulen, W., Yeh, H., Forrester, K., Sturzbecher, H. W., Hoeijmakers, J. H., and Harris, C. C. (1995) *Cancer Res.* **55,** 6012–6016
20. Chirillo, P., Pagano, S., Natoli, G., Puri, P. L., Burgio, V. L., Balsano, C., and Levrero, M. (1997) *Proc. Natl. Acad. Sci. U. S. A.* **94,** 8162–8167
21. Terradillos, O., Pollicino, T., Lecoeur, H., Tripodi, M., Gougeon, M. L., Tiollais, P., and Buendia, M. A. (1998) *Oncogene* **17,** 2115–2123
22. Ueda, H., Ullrich, S. J., Gangemi, J. D., Kappel, C. A., Ngo, L., Feitelson, M. A., and Jay, G. (1995) *Nat. Genet.* **9,** 41–47
23. Elmore, L. W., Hancock, A. R., Chang, S. F., Wang, X. W., Chang, S., Callahan, C. P., Geller, D. A., Will, H., and Harris, C. C. (1997) *Proc. Natl. Acad. Sci. U. S. A.* **94,** 14707–14712
24. Takada, S., Kaneniwa, N., Tsuchida, N., and Koike, K. (1997) *Oncogene* **15,** 1895–1901
25. Su, Q., Schroder, C. H., Otto, G., and Bannasch, P. (2000) *Mutat. Res.* **462,** 365–380
26. Butel, J. S. (2000) *Carcinogenesis* **21,** 405–426
27. He, T. C., Zhou, S., da Costa, L. T., Yu, J., Kinzler, K. W., and Vogelstein, B. (1998) *Proc. Natl. Acad. Sci. U. S. A.* **95,** 2509–2514
28. Lee, C. G., Ren, J., Cheong, I. S., Ban, K. H., Ooi, L. L., Yong Tan, S., Kan, A., Nuchprayoon, I., Jin, R., Lee, K. H., Choti, M., and Lee, L. A. (2003) *Oncogene* **22,** 2592–2603
29. Su, Q., Schroder, C. H., Hofmann, W. J., Otto, G., Pichlmayr, R., and Bannasch, P. (1998) *Hepatology* **27,** 1109–1120
30. Shirakata, Y., and Koike, K. (2003) *J. Biol. Chem.* **278,** 22071–22078
31. Yun, C., Lee, J. H., Park, H., Jin, Y. M., Park, S., Park, K., and Cho, H. (2000) *Oncogene* **19,** 5163–5172
32. Pollicino, T., Terradillos, O., Lecoeur, H., Gougeon, M. L., and Buendia, M. A. (1998) *Biomed. Pharmacother.* **52,** 363–368
33. de Vries, A., van Oostrom, C. T., Hofhuis, F. M., Dortant, P. M., Berg, R. J., de Gruijl, F. R., Wester, P. W., van Kreijl, C. F., Capel, P. J., van Steeg, H., and Verbeek, S. J. (1995) *Nature* **377,** 169–173
34. Sands, A. T., Abuin, A., Sanchez, A., Conti, C. J., and Bradley, A. (1995) *Nature* **377,** 162–165
35. Chresta, C. M., Arriola, E. L., and Hickman, J. A. (1996) *Behring. Inst. Mitt.* **97,** 232–240
36. Nomura, T., Lin, Y., Dorjsuren, D., Ohno, S., Yamashita, T., and Murakami, S. (1999) *Biochim. Biophys. Acta* **1453,** 330–340
37. Hoare, J., Henkler, F., Dowling, J. J., Errington, W., Goldin, R. D., Fish, D., and McGarvey, M. J. (2001) *J. Med. Virol.* **64,** 419–426
38. Doria, M., Klein, N., Lucito, R., and Schneider, R. J. (1995) *EMBO J.* **14,** 4747–4757
39. Shintani, Y., Yotsuyanagi, H., Moriya, K., Fujie, H., Tsutsumi, T., Kanegae, Y., Kimura, S., Saito, I., and Koike, K. (1999) *J. Gen. Virol.* **80,** 3257–3265
40. Levine, A. J. (1997) *Cell* **88,** 323–331
41. el-Deiry, W. S. (1998) *Semin. Cancer Biol.* **8,** 345–357
42. Niculescu, A. B., III, Chen, X., Smeets, M., Hengst, L., Prives, C., and Reed, S. I. (1998) *Mol. Cell. Biol.* **18,** 629–643
43. Roninson, I. B. (2002) *Cancer Lett.* **179,** 1–14
44. Wang, X. W., Zhan, Q., Coursen, J. D., Khan, M. A., Kontny, H. U., Yu, L., Hollander, M. C., O'Connor, P. M., Fornace, A. J., Jr., and Harris, C. C. (1999) *Proc. Natl. Acad. Sci. U. S. A.* **96,** 3706–3711
45. Bunz, F., Dutriaux, A., Lengauer, C., Waldman, T., Zhou, S., Brown, J. P., Sedivy, J. M., Kinzler, K. W., and Vogelstein, B. (1998) *Science* **282,** 1497–1501
46. Taylor, W. R., DePrimo, S. E., Agarwal, A., Agarwal, M. L., Schonthal, A. H., Katula, K. S., and Stark, G. R. (1999) *Mol. Biol. Cell* **10,** 3607–3622
47. Bellamy, C. O., Clarke, A. R., Wyllie, A. H., and Harrison, D. J. (1997) *FASEB J.* **11,** 591–599
48. Prost, S., Ford, J. M., Taylor, C., Doig, J., and Harrison, D. J. (1998) *J. Biol. Chem.* **273,** 33327–33332
49. Arbuthnot, P., Capovilla, A., and Kew, M. (2000) *J. Gastroenterol. Hepatol.* **15,** 357–368
50. Jia, L., Wang, X. W., and Harris, C. C. (1999) *Int. J. Cancer* **80,** 875–879
51. Su, F., and Schneider, R. J. (1997) *Proc. Natl. Acad. Sci. U. S. A.* **94,** 8744–8749
52. Benn, J., and Schneider, R. J. (1995) *Proc. Natl. Acad. Sci. U. S. A.* **92,** 11215–11219
53. Lau, J. Y., Xie, X., Lai, M. M., and Wu, P. C. (1998) *Semin. Liver Dis.* **18,** 169–176
54. Fischer, M., Runkel, L., and Schaller, H. (1995) *Virus Genes* **10,** 99–102
55. Hu, Z., Zhang, Z., Doo, E., Coux, O., Goldberg, A. L., and Liang, T. J. (1999) *J. Virol.* **73,** 7231–7240
56. Sirma, H., Weil, R., Rosmorduc, O., Urban, S., Israel, A., Kremsdorf, D., and Brechot, C. (1998) *Oncogene* **16,** 2051–2063
57. Chen, X., Zhang, Y., Douglas, L., and Zhou, P. (2001) *J. Biol. Chem.* **276,** 48175–48182
58. Bergametti, F., Sitterlin, D., and Transy, C. (2002) *J. Virol.* **76,** 6495–6501
59. Nag, A., Datta, A., Yoo, K., Bhattacharyya, D., Chakrabortty, A., Wang, X., Slagle, B. L., Costa, R. H., and Raychaudhuri, P. (2001) *J. Virol.* **75,** 10383–10392
60. Abramic, M., Levine, A. S., and Protic, M. (1991) *J. Biol. Chem.* **266,** 22493–22500
61. Hwang, B. J., Toering, S., Francke, U., and Chu, G. (1998) *Mol. Cell. Biol.* **18,** 4391–4399
62. Tang, J. Y., Hwang, B. J., Ford, J. M., Hanawalt, P. C., and Chu, G. (2000) *Mol. Cell* **5,** 737–744
63. Lee, T. H., Elledge, S. J., and Butel, J. S. (1995) *J. Virol.* **69,** 1107–1114
64. Qadri, I., Conaway, J. W., Conaway, R. C., Schaack, J., and Siddiqui, A. (1996) *Proc. Natl. Acad. Sci. U. S. A.* **93,** 10578–10583
65. Bontron, S., Lin-Marq, N., and Strubin, M. (2002) *J. Biol. Chem.* **277,** 38847–38854
66. Kwun, H. J., and Jang, K. L. (2004) *Nucleic Acids Res.* **32,** 2202–2213
67. Picksley, S. M., and Lane, D. P. (1993) *BioEssays* **15,** 689–690
68. Chen, J., Lin, J., and Levine, A. J. (1995) *Mol. Med.* **1,** 142–152
69. Haupt, Y., Maya, R., Kazaz, A., and Oren, M. (1997) *Nature* **387,** 296–299
70. Kubbutat, M. H., Jones, S. N., and Vousden, K. H. (1997) *Nature* **387,** 299–303
71. Wang, X. W., Yeh, H., Schaeffer, L., Roy, R., Moncollin, V., Egly, J. M., Wang, Z., Freidberg, E. C., Evans, M. K., Taffe, B. G., Bohr, V. A., Weeda, G., Hoeijmakers, J. H. J., Forrester, K., and Harris, C. C. (1995) *Nat. Genet.* **10,** 188–195
72. Vousden, K. H., and Lu, X. (2002) *Nat. Rev. Cancer* **2,** 594–604
73. Fridman, J. S., and Lowe, S. W. (2003) *Oncogene* **22,** 9030–9040
74. Chisari, F. V., and Ferrari, C. (1995) *Springer Semin. Immunopathol.* **17,** 261–281
75. Teodoro, J. G., and Branton, P. E. (1997) *J. Virol.* **71,** 1739–1746